Electronic Supplementary Material (ESI) for Soft Matter.
This journal is © The Royal Society of Chemistry 2023

Supplementary Information

Kinetics of Evaporation of Colloidal Dispersion Drops on Inclined Surfaces

Sankar Hariharan, Sumesh P Thampi[‡] and Madivala G. Basavaraj [*]

Polymer Engineering and Colloid Science Lab, Department of Chemical Engineering, Indian Institute of Technology Madras, Chennai 600036, Tamil Nadu, India
Corresponding authors: [‡]sumesh@iitm.ac.in; [*]basa@iitm.ac.in

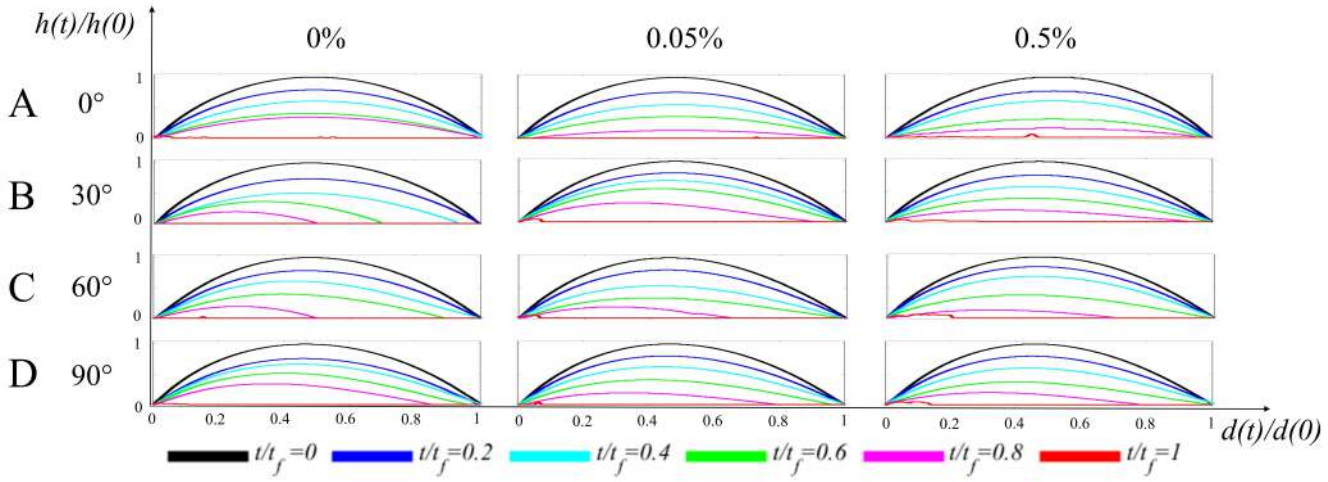

Fig. S1 The temporal evolution ($t/t_f = 0, 0.2, 0.4, 0.6, 0.8$ and 1.0) of the profile of the drying 2 μL drop for various inclinations and particle concentrations

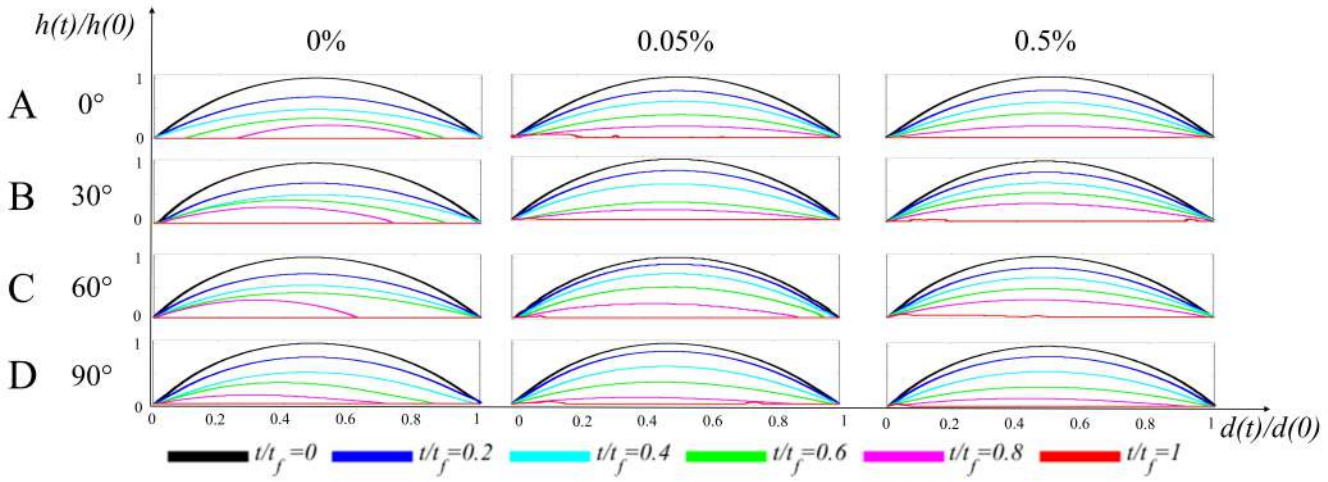

Fig. S2 The temporal evolution ($t/t_f = 0, 0.2, 0.4, 0.6, 0.8$ and 1.0) of the profile of the drying 1 μL drop for various inclinations and particle concentrations

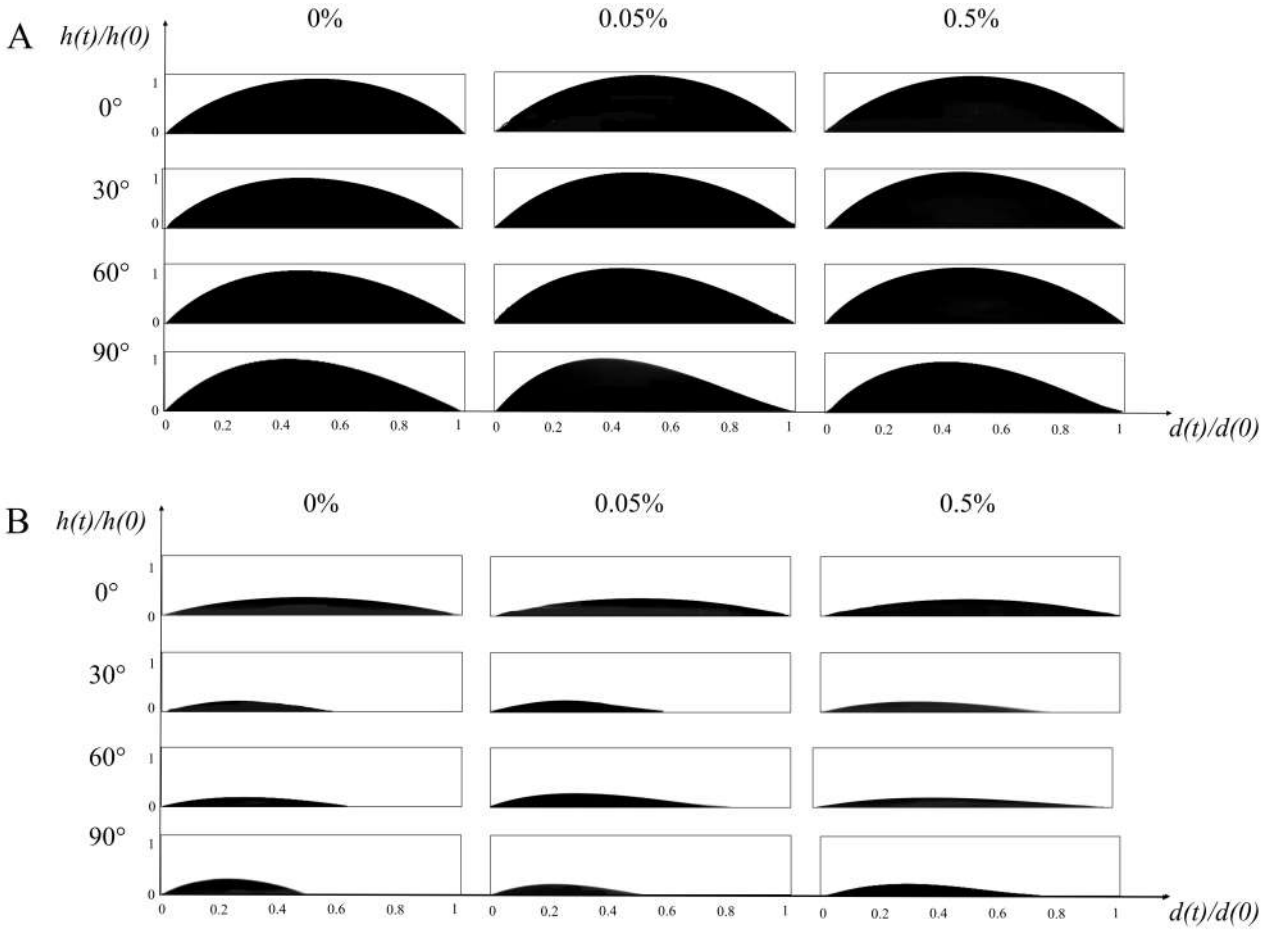

Fig. S3 The side view of the drop of volume 5 μL for various inclinations and particle concentrations obtained from the camera attached to the goniometer at (A) $t/t_f = 0$ and (B) $t/t_f = 0.8$

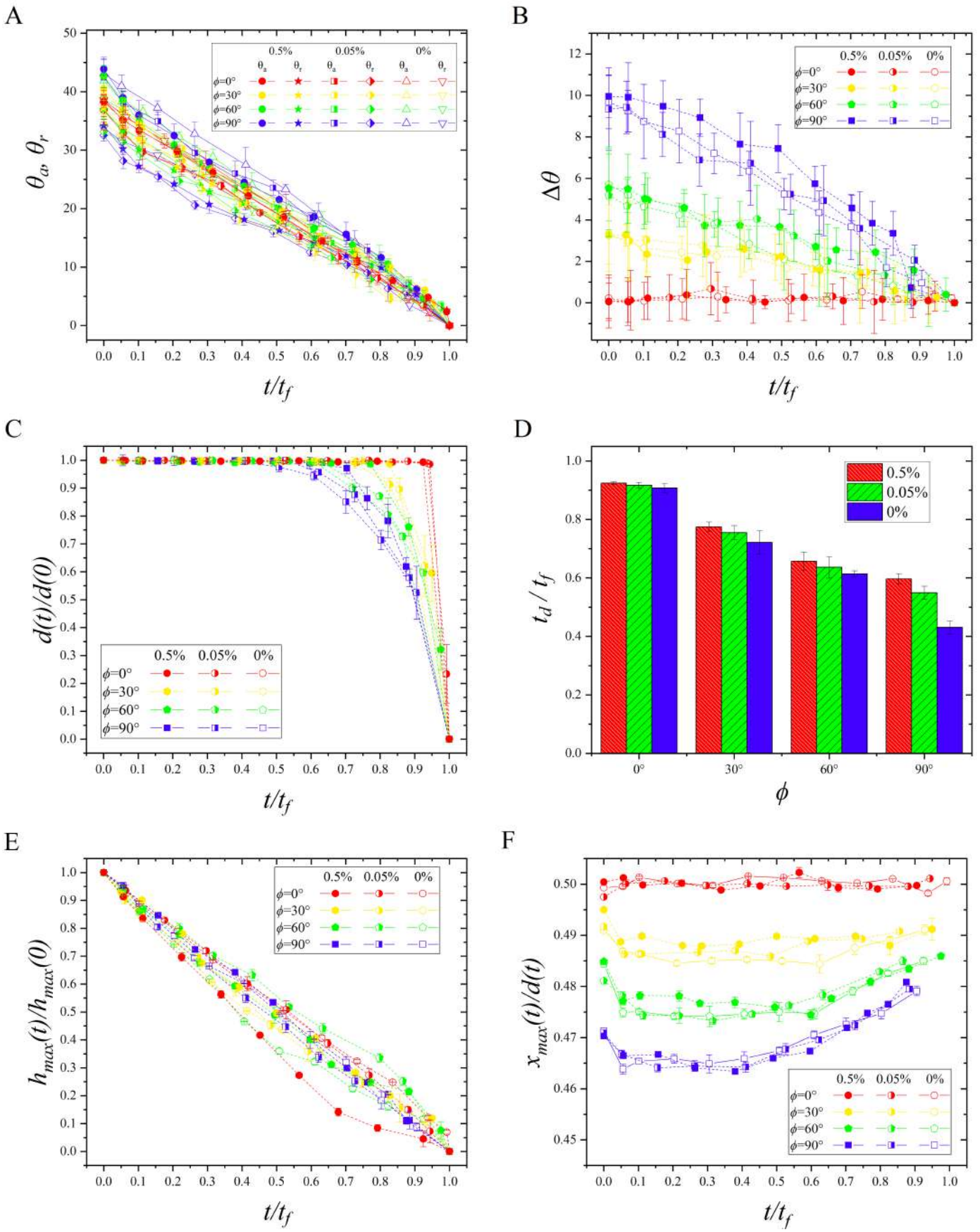

Fig. S4 Temporal evolution of geometric parameters of an evaporating 2 μL drop at various particle loading (0 wt.% to 0.5 wt.%) and at different substrate inclinations (ϕ): (A) Contact angles at the advancing side, θ_a and the receding side, θ_r; (B) The difference between the contact angle at the advancing side and the receding side; (C) Diameter of the contact line; (D) Depinning time as a function of substrate inclination; (E) Maximum height of the drop; (F) Location of the maximum height measured from advancing side

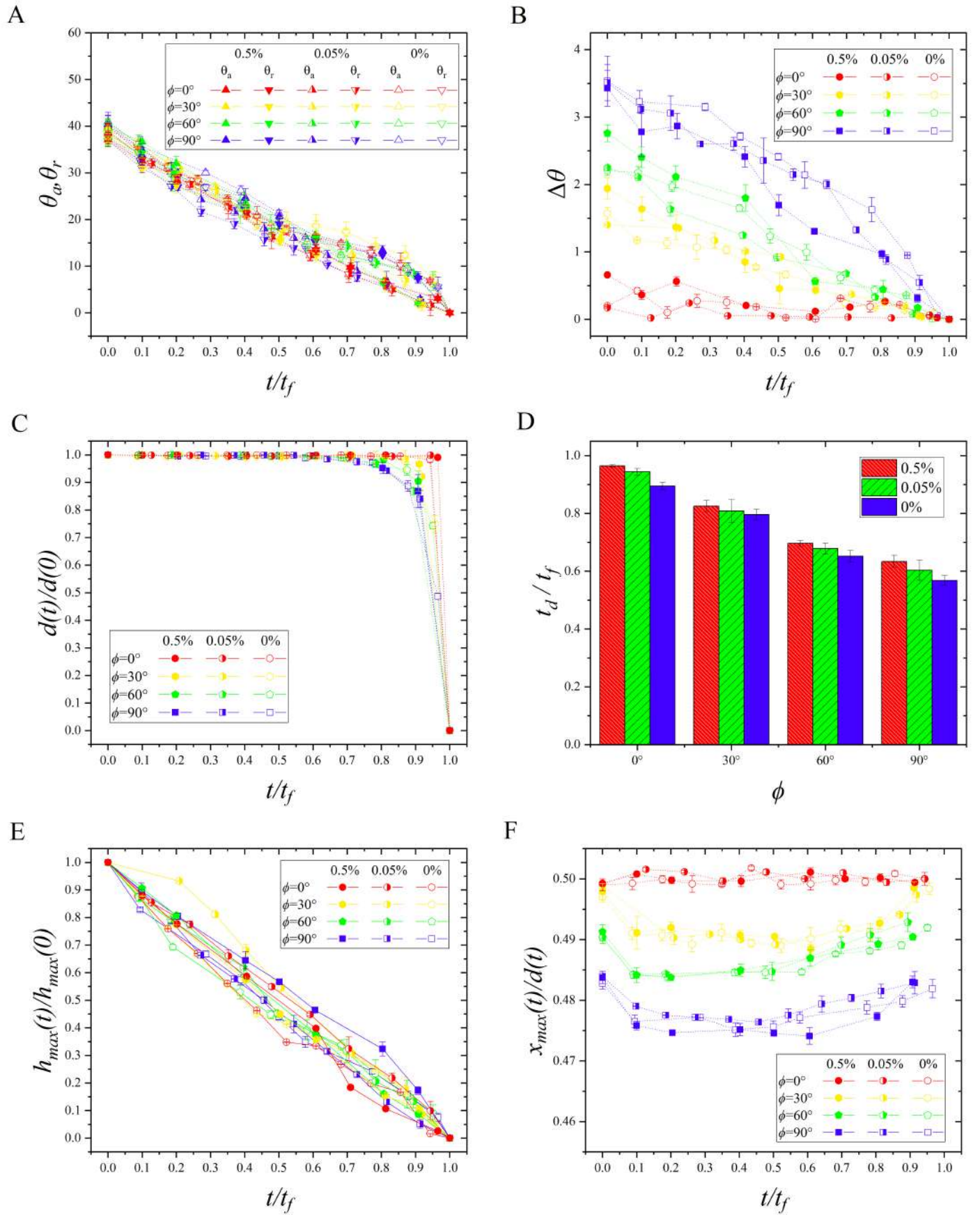

Fig. S5 Temporal evolution of geometric parameters of an evaporating 1 μL drop at various particle loading (0 wt.% to 0.5 wt.%) and at different substrate inclinations (ϕ): (A) Contact angles at the advancing side, θ_a and the receding side, θ_r; (B) The difference between the contact angle at the advancing side and the receding side; (C) Diameter of the contact line; (D) Depinning time as a function of substrate inclination; (E) Maximum height of the drop; (F) Location of the maximum height measured from advancing side

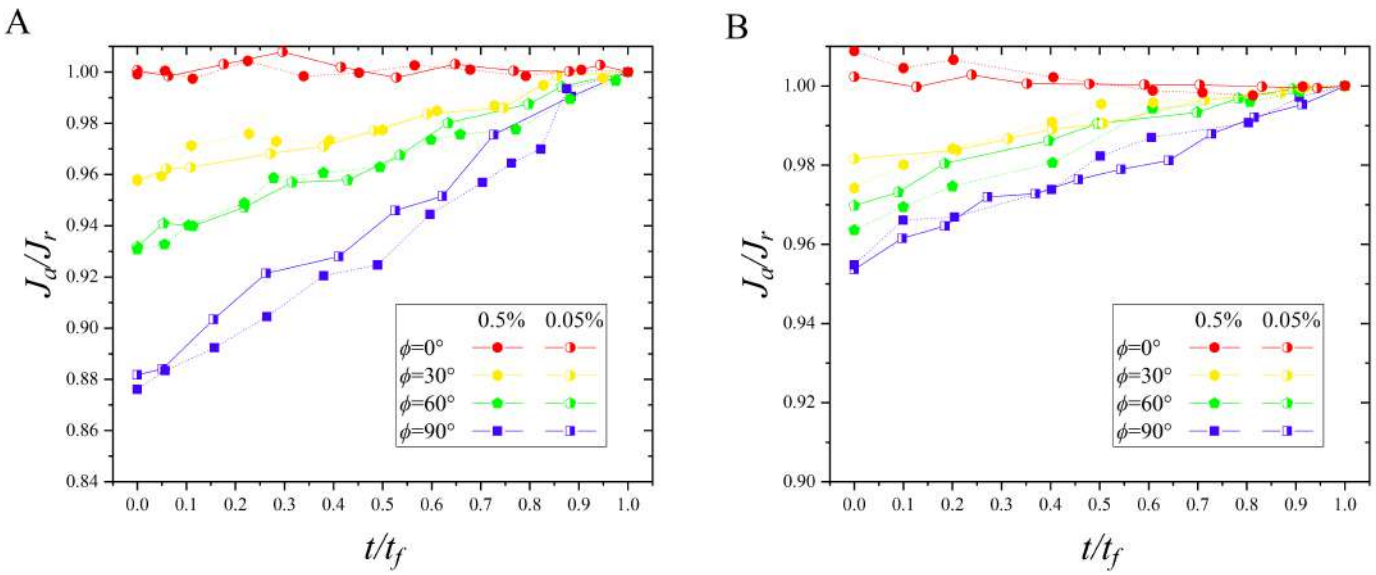

Fig. S6 Ratio of the evaporative mass flux at the advancing side to that at the receding side as a function of time for (A) 2 μL and (B) 1 μL drops dried on substrates at different orientations and particle loading

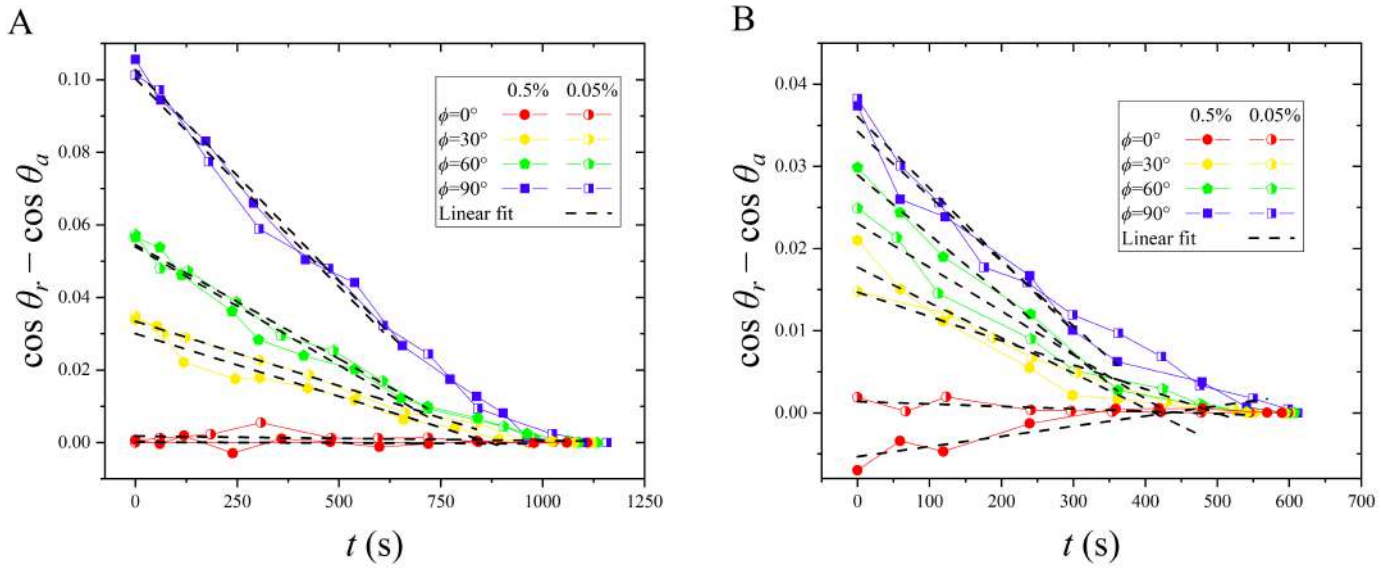

Fig. S7 The difference in the cosine of the contact angle between the receding side and the advancing side as a function of time for (A) 2 μL drop and (B) 1 μL drop dried on substrates at different orientations and particle loading.The linear fit to Equation 7 (in the manuscript) is shown as dashed lines

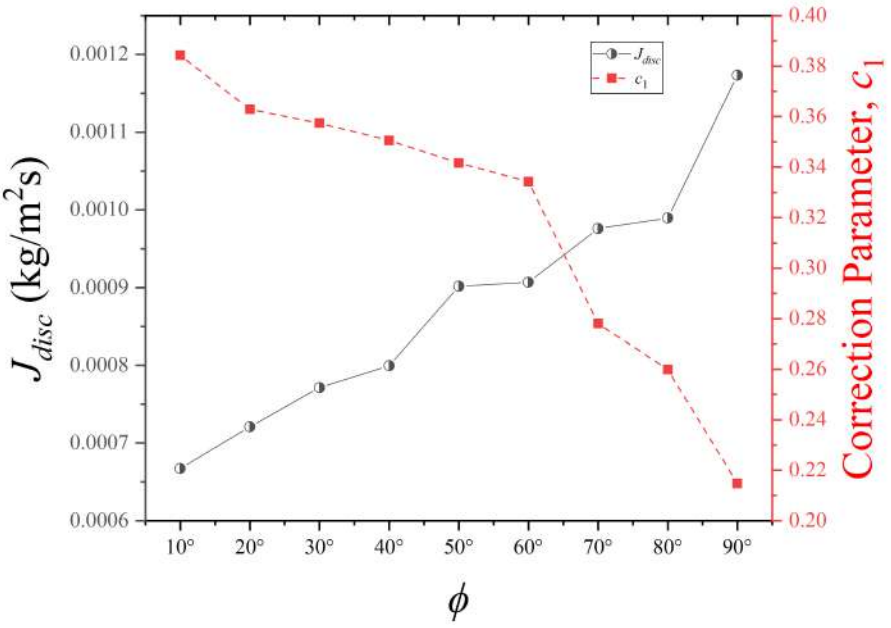

Fig. S8 Variation of the evaporative flux J_{disc} and correction parameter c_1 with angle of inclination for a 5 μL drop with an initial particle concentration of 0.05 %

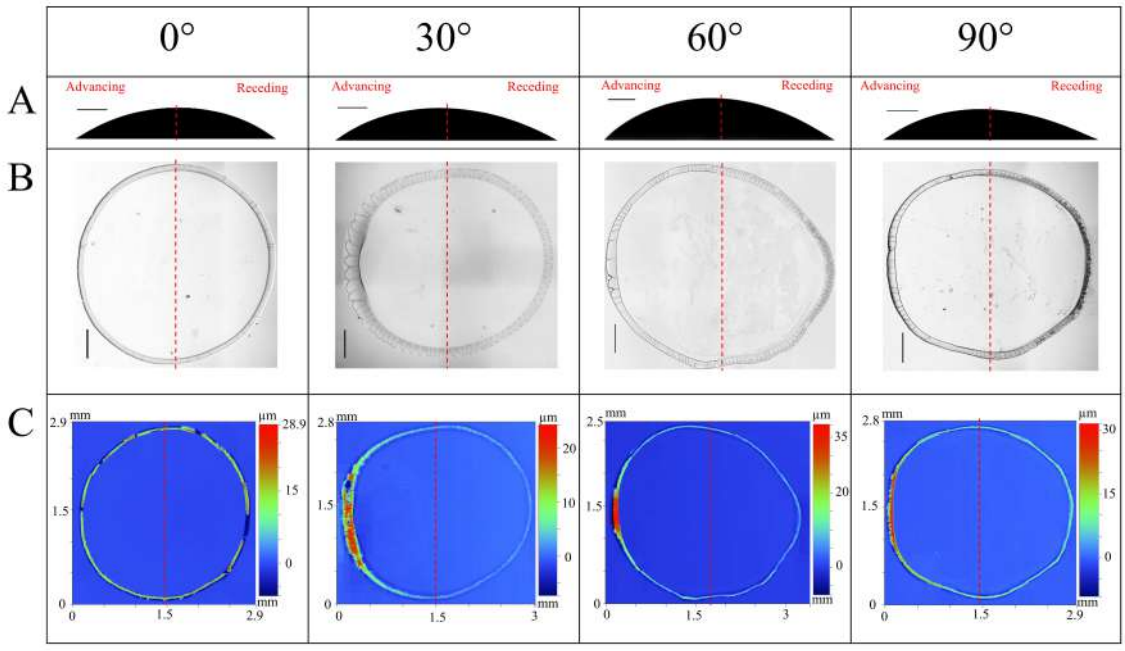

Fig. S9 (A) The side view at t/t_f=0 (scale bar= 250 μm), (B) Microscope image of the final dried deposits at t/t_f=1 (scale bar = 250 μm), and (C) Optical surface profiles of the dried deposits after the completion of drying, at ϕ= 0°, 30°, 60° and 90° for a 2 μL drop with an initial particle concentration of 0.5%

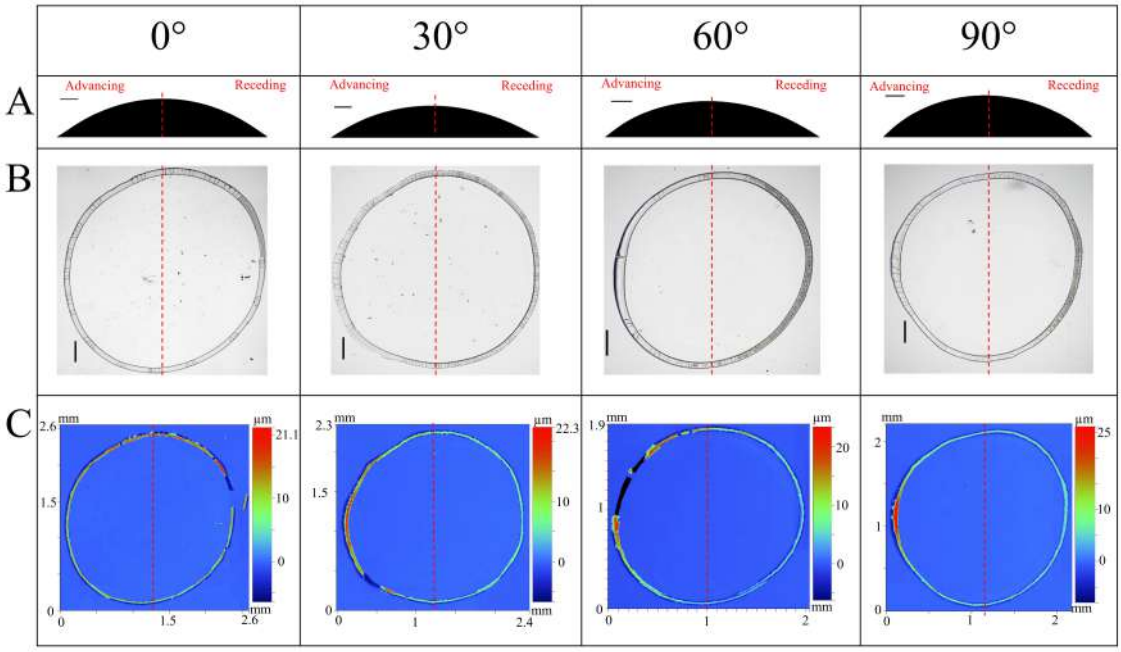

Fig. S10 (A) The side view at t/t_f=0 (scale bar= 200 μm), (B) Microscope image of the final dried deposits at t/t_f=1 (scale bar = 200 μm), and (C) Optical surface profiles of the dried deposits after the completion of drying, at ϕ= 0°, 30°, 60° and 90° for a 1 μL drop with an initial particle concentration of 0.5%